

Supplemental Material

Supplemental Section for

Protection of cystinotic mice by kidney-specific megalin ablation supports an endocytosis-based mechanism for nephropathic cystinosis progression.

Virginie Janssens¹, Héloïse P. Gaide Chevronnay¹, Sandrine Marie², Marie-Françoise Vincent², Patrick Van Der Smissen¹, Nathalie Nevo³, Seppo Vainio⁴, Rikke Nielsen⁵, Erik I. Christensen⁵, François Jouret⁶, Corinne Antignac³, Christophe E. Pierreux^{1*}, Pierre J. Courtoy^{1*}.

Table of Contents

Supplementary Methods	3
Semi-thin sections and electron microscopy	3
RT-PCR	3
Supplementary Figures	4
Supplementary figure 1 : Time-course of body and kidney weight	4
Supplementary figure 2 : Megalin ablation in Ctns ^{-/-} kidneys selectively prevents cystine accumulation (complementary to Figure 2A)	5
Supplementary figure 3 : Megalin ablation in Ctns ^{-/-} kidneys prevents cystine crystal deposition: gallery of images (complementary to Figure 2B).....	6
Supplementary figure 4 : Toluidine-stained plastic sections of Ctns ^{-/-} vs double KO kidneys	7
Supplementary figure 5 : Electron microscopy	8
Supplementary figure 6 : Diffuse mottled appearance resulting from loss of transporter expression in Ctns ^{-/-} PCTs contrasts with large areas of inflammatory remodelling in double KO. A. Low power cortical views. B. Extended views of whole kidney sections (complementary to Figure 5).....	9
Supplementary figure 7 : RT-PCR of megalin, cubilin, NaPi-IIa and SGLT-2....	12
Supplementary References	13

Supplementary Methods

Semi-thin sections and electron microscopy

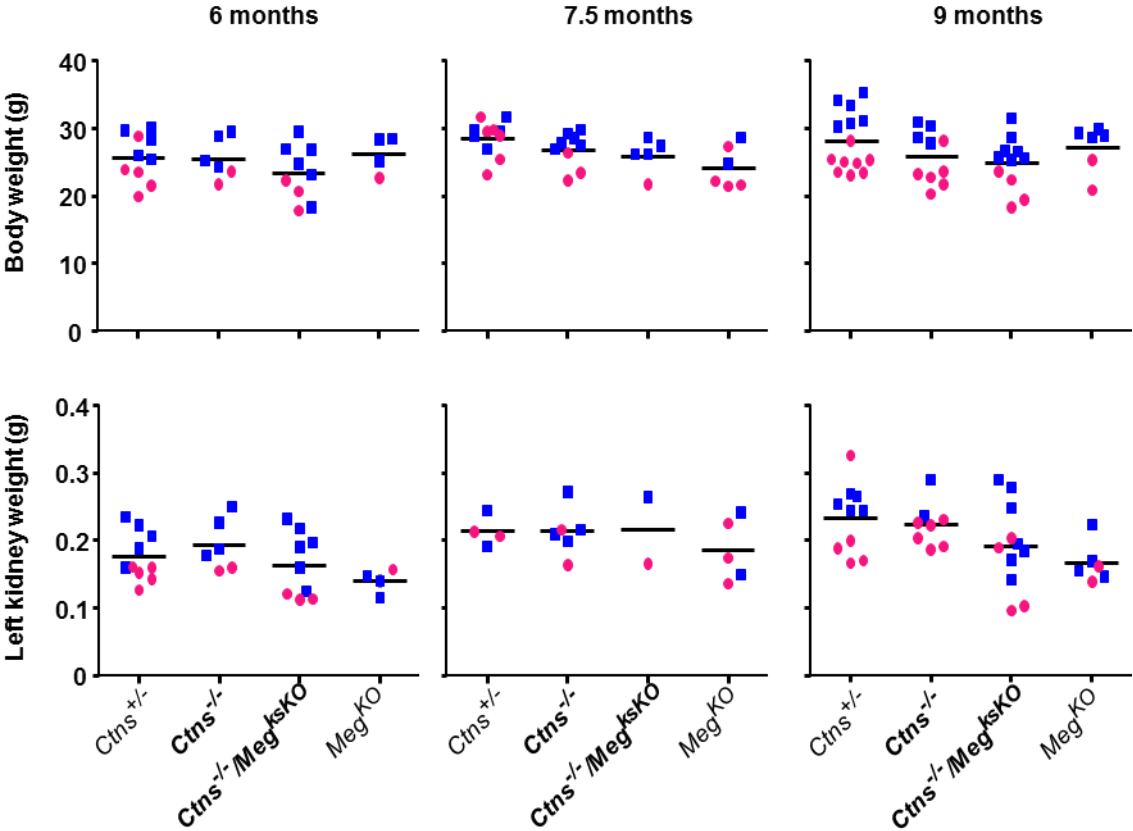
Kidneys were perfusion-fixed *in situ* with 4% formaldehyde in 0.1 M phosphate buffer, pH 7.4 as above, then excised and small blocks of cortices were immediately post-fixed in 4% formaldehyde supplemented by 0.5% (v/v) glutaraldehyde in 0.1 M cacodylate buffer, pH 7.4 at 4°C, overnight in rotating vessels. Samples were further processed exactly as described in [1]. Briefly, blocks were further osmicated, stained “en bloc” with uranyl acetate, dehydrated and embedded in Spurr. Semi-thin sections (1-microm, nominal) were collected on glass slides and stained with toluidine blue. Ultrathin sectioning (70-nm nominal) was guided by toluidine-stained semi-thin sections. Ultrathin sections were collected on 400-mesh rhodanium grids, sequentially contrasted with uranyl and lead, and examined in a FEI CM12 electron microscope operating at 80 kV.

RT-PCR

Total RNA was extracted (SV total RNA isolation system; Promega). Aliquots of 500 ng RNA were reverse-transcribed by M-MLV reverse transcriptase (Invitrogen) with the random hexamers protocol (primer random p(dN)₆, Roche). Primer sequences for hypoxanthine phosphoribosyltransferase 1 (HPRT-1; used as house-keeping gene), glyceraldehyde 3-phosphate dehydrogenase (GAPDH; used to test primer efficiency), cubilin, SGLT-2 and NaPi-IIa are described in Gaide Chevronnay et al. 2014. [1] Real-time qPCR was performed as described [2] in presence of 250 mM of specific primers with Kappa SYBR Fast qPCR Master Mix (Kapa Biosystems) on a CFX96 touch real-time PCR Detection System (Bio-Rad). Data were analyzed using the $\Delta\Delta CT$ method, using HPRT-1 as internal standard, and presented as fold-change.

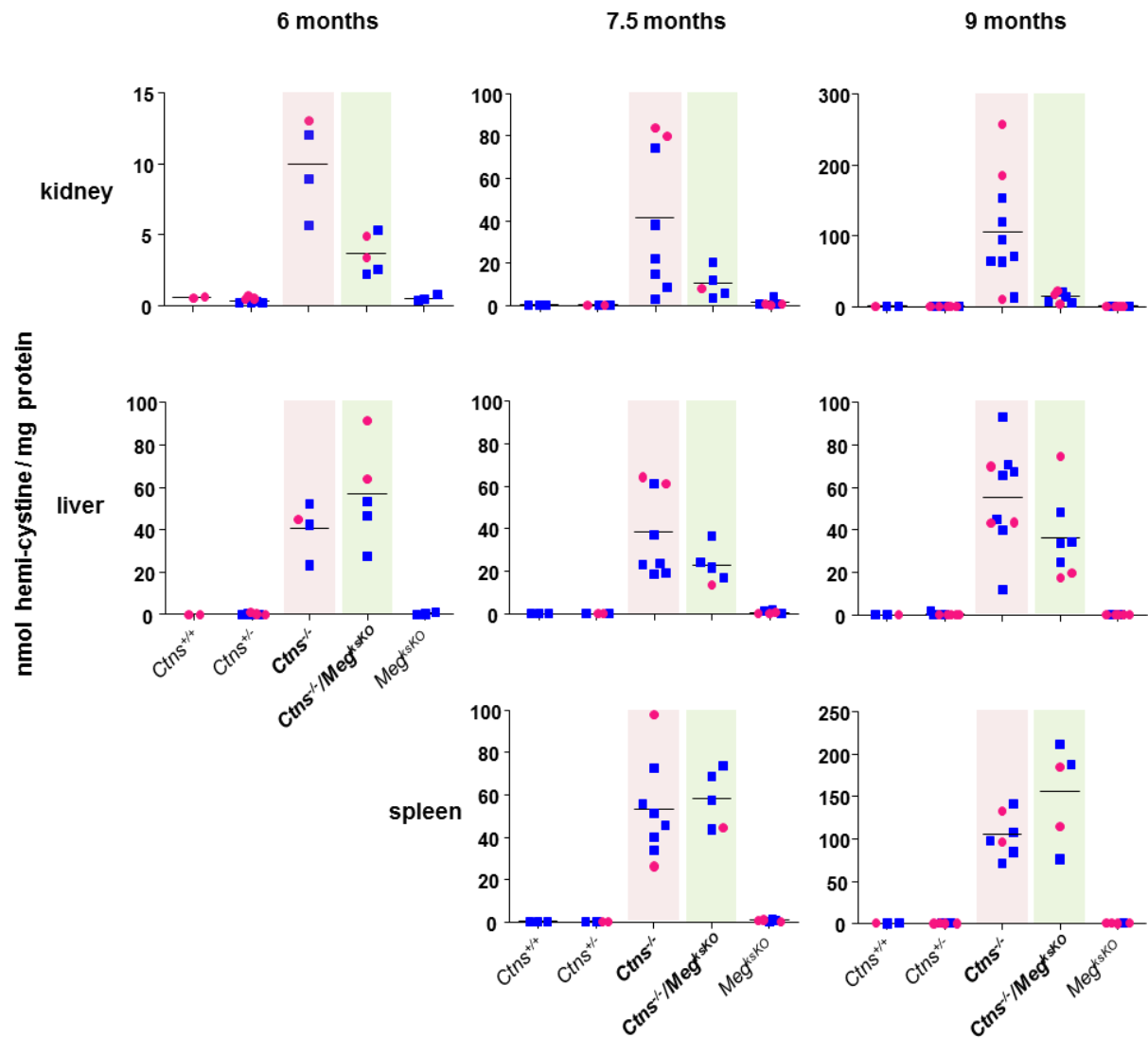
Supplementary Figures

Supplementary figure 1



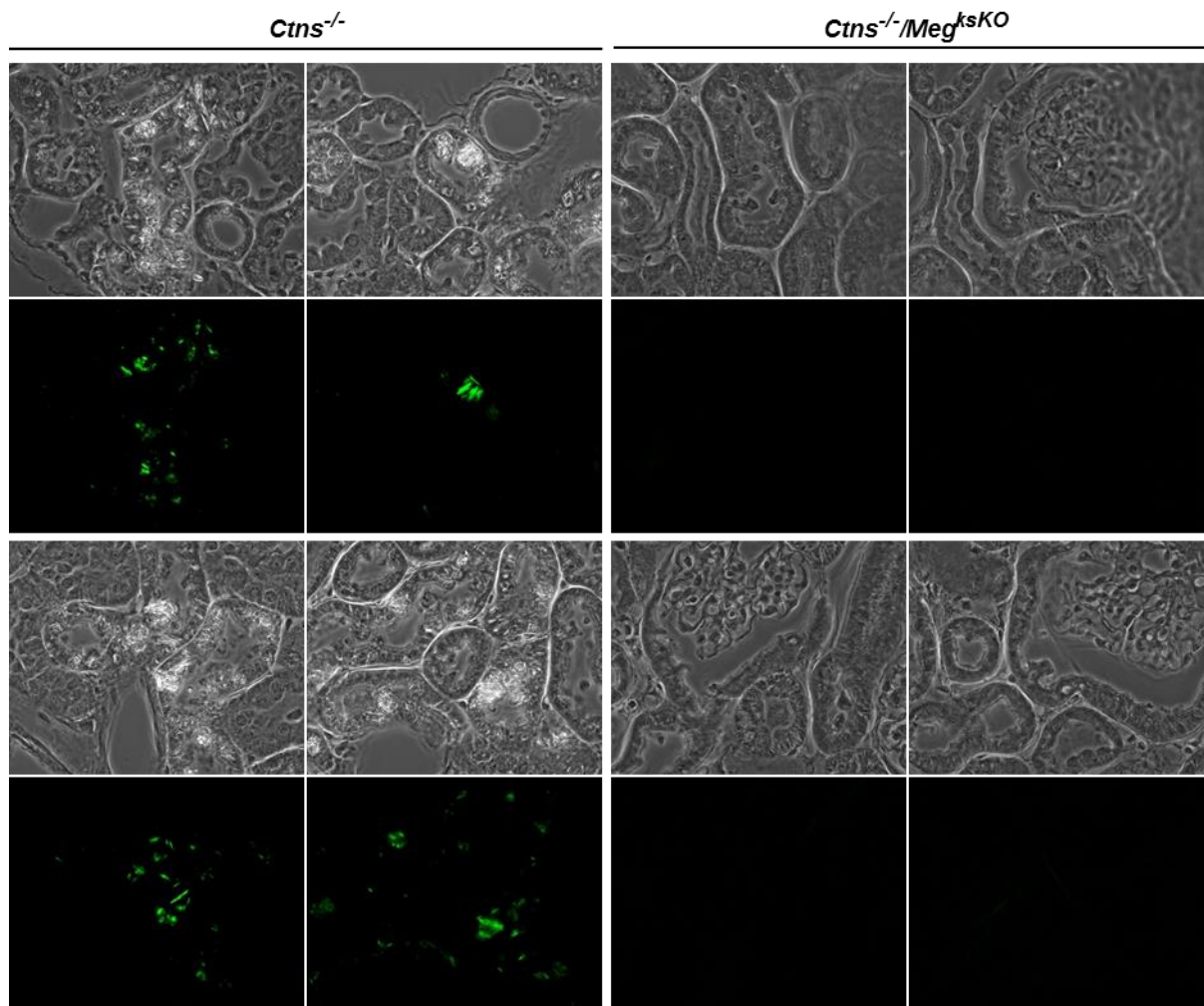
Body and kidney weights. Mice and left kidneys (not fixed by perfusion; when saved) were weighed at the time of sacrifice (males, blue squares; females, red disks). There was no significant difference between any genotype in our colony.

Supplementary figure 2 (complementary to Figure 2A)



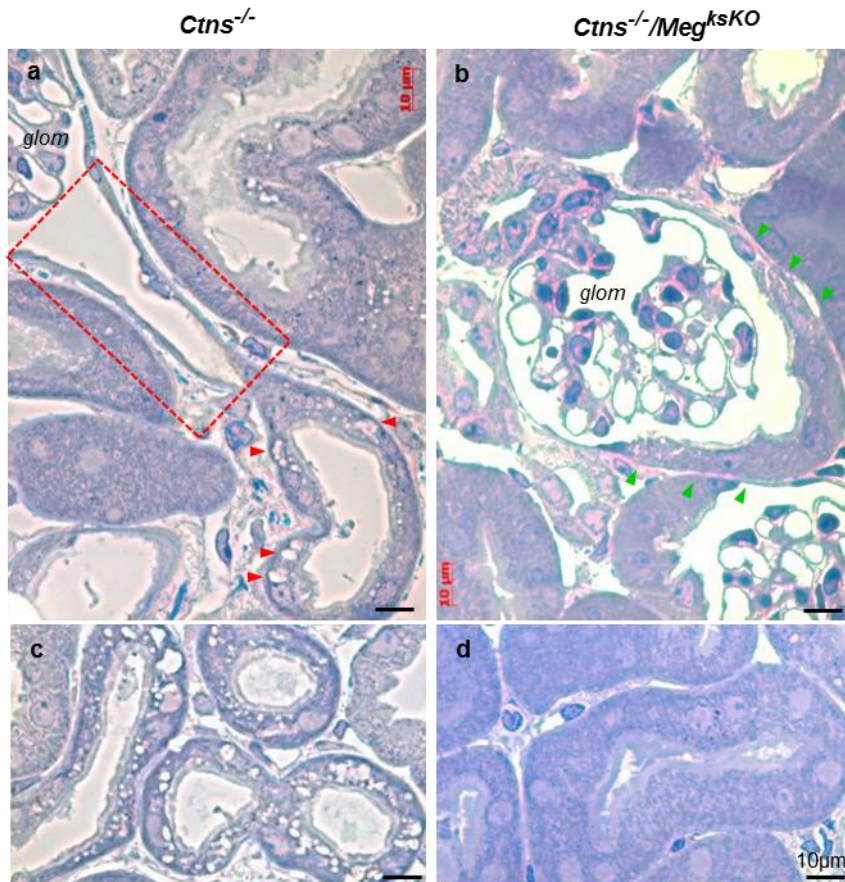
Megalín ablation in *Ctns*^{-/-} kidneys selectively prevents cystine accumulation: time-course in comparison with liver and spleen. Time-course of cystine content in kidneys, liver and spleen of 6, 7.5 and 9 months-old mice of the indicated genotypes (males, blue squares; females, red disks). In *Ctns*^{-/-} kidneys, median cystine content increases exponentially between 6 and 9 months (note difference of ordinate scale). In double KO kidneys, content is moderately increased yet remains rather low at all time-points. In contrast, liver and spleen content in *Ctns*^{-/-} and double KO mice, serving as positive controls for cystinosin deletion, show high cystine levels irrespective of megalín ablation. Data on spleen at 6 months are not available.

Supplementary figure 3 ([complementary to Figure 2B](#))



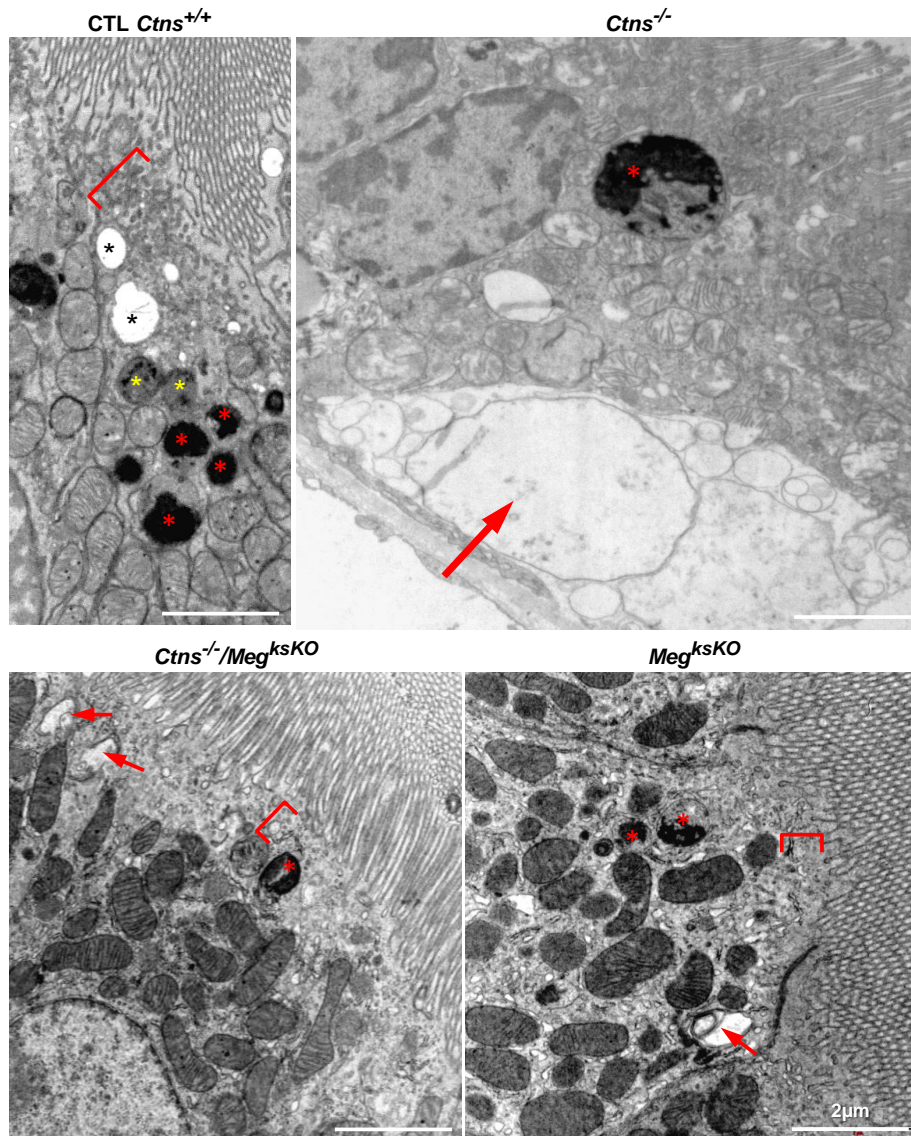
Megalin ablation in *Ctns*^{-/-} kidneys prevents cystine crystal deposition: gallery of images as in Figure 3B.

Supplementary figure 4



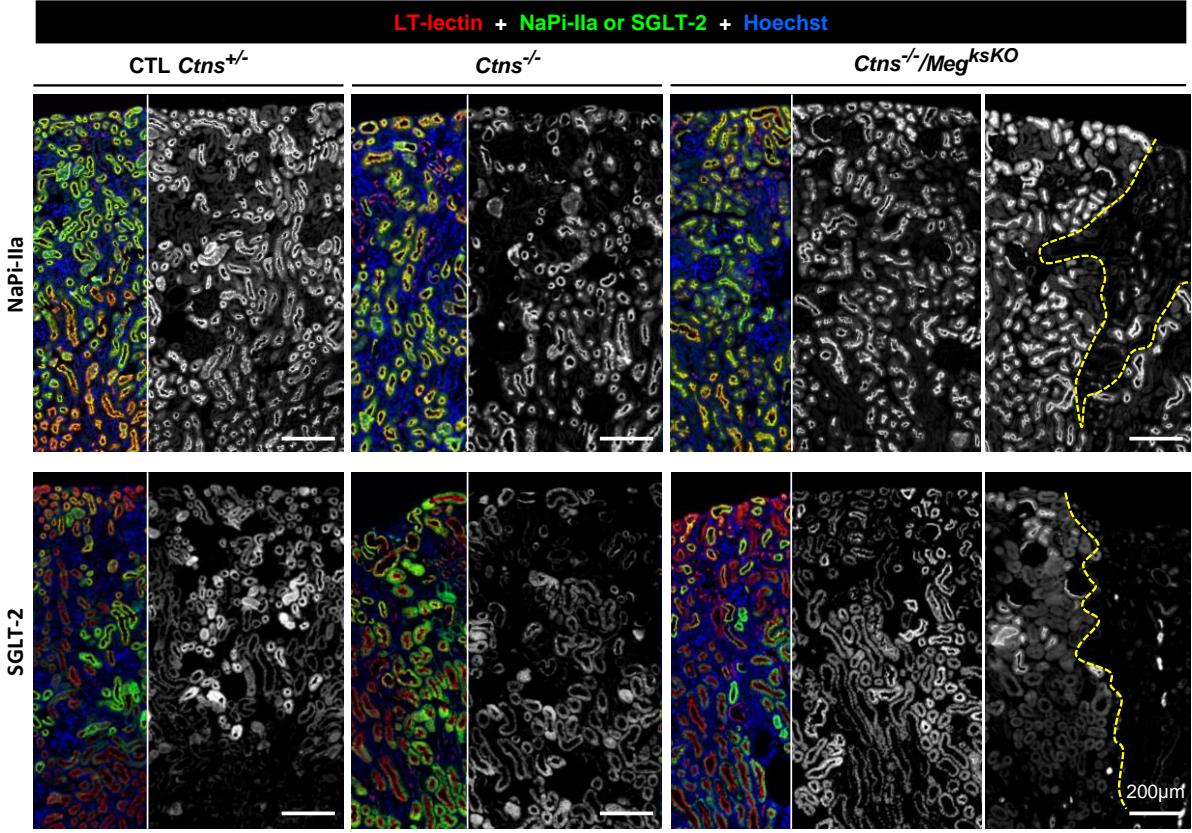
Toluidine-stained plastic sections of *Ctns*^{-/-} vs double KO kidneys (9 months). Upper panels (a-b), GTJs; lower panels (c-d), clusters of proximal tubules; all at identical magnification. In the upper panel, notice at left swan-neck lesion (in red box) and structural abnormalities in continuing S1 PCTs (red arrowheads) of *Ctns*^{-/-} kidney, contrasting with preservation in double KO (green arrowheads). In lower panel, notice extensively vacuolated and much thinner *Ctns*^{-/-} PCTs as compared with double KO.

Supplementary figure 5

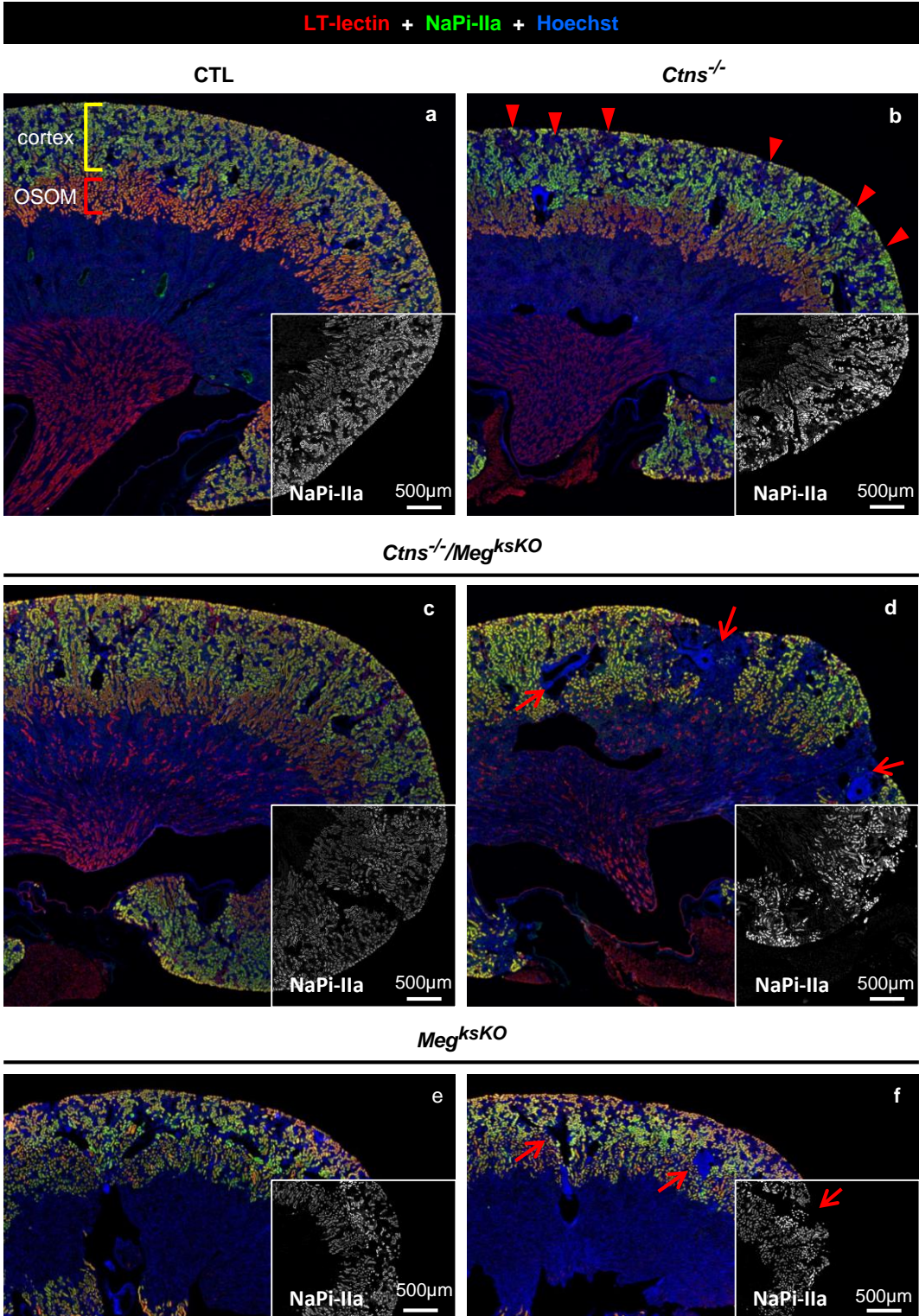


Electron microscopy (6 months). In this favorable view of a control PCT, notice the remarkable stratification of the apical endocytic apparatus. Immediately under the brush border is a dense layer exclusively made of packed dense apical tubules (recycling endosomes; bracket). Below are apical vacuoles (sorting endosomes, two black asterisks), then intermediate organelles resulting from fusion between late endosomes and lysosomes (endo-lysosomes, two yellow asterisks), then a cluster of dense bodies (secondary lysosomes, four red asterisks). In this *Ctns*^{-/-} kidney, a partially preserved PCT with a huge lysosome (red asterisk) lies over a dead PCT still in contact with the tubular basement membrane (large arrow). In double KO as in single megalin KO kidneys, PTCs are overall well preserved, except for the absence of dense apical (recycling) tubules (indicated by brackets) and fewer small lysosomes (red asterisks). Arrows point to autophagic structures. All equal scale bars at 2 microm.

Supplementary figure 6A (complementary to Figure 5)

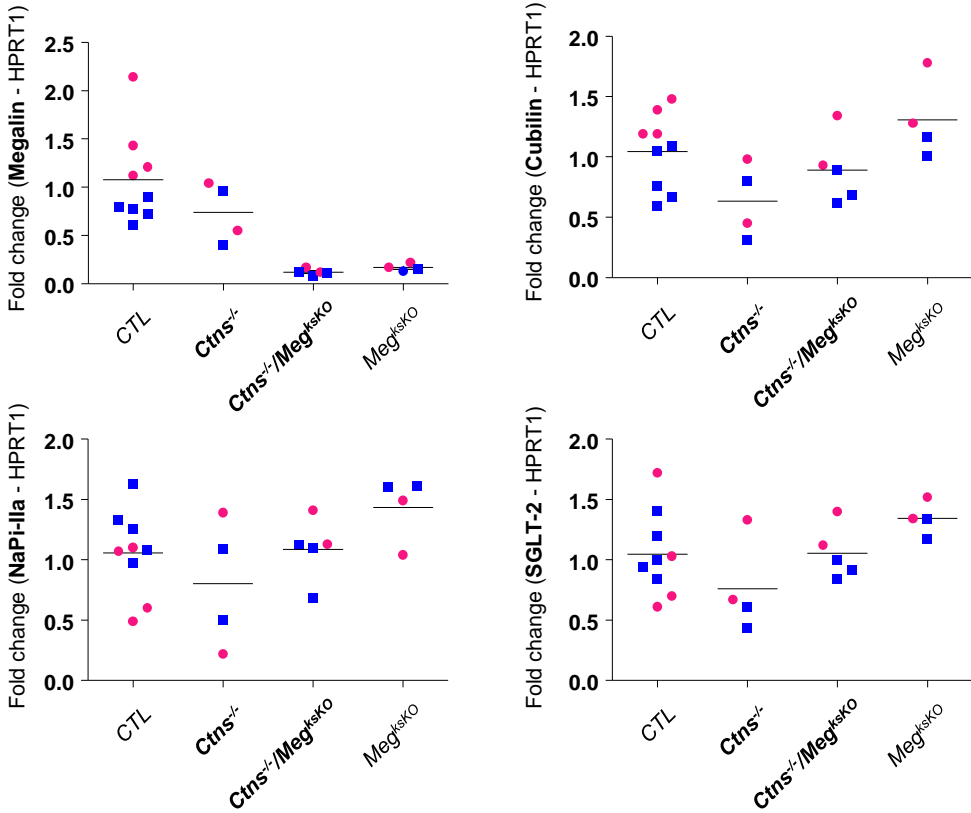


Supplementary figure 6B (complementary to Figure 5)



Diffuse mottled appearance resulting from loss of transporter expression in $Ctns^{-/-}$ PCTs contrasts with large areas of inflammatory remodelling in double KO. **A.** Low power views across the cortex at 9 months of age. Whole kidney sections were processed for triple fluorescence labelling to compare NaPi-IIa or SGLT-2 (both in green) to LT-lectin (red) and nuclei (Hoechst, blue) and presented at left of each pair in triple color, or limited at right to NaPi-IIa (upper panel) or SGLT-2 (lower panel) presented in black and white. **B.** Extended views of whole kidney sections showing triple labelling with NaPi-IIa (triple color) or only NaPi-IIa (black/white; continuing field). In WT (a), LT-lectin labeling encompasses the entire OSOM (thus including S3; red only) whereas NaPi-IIa is sharply limited to cortex (together with LT-lectin, thus yellow). In $Ctns^{-/-}$ (b), arrowheads point to mottled appearance. Two examples illustrate the variable pattern of double KO (c,d) and single *Meg* KO (e,f). At right (d,f), arrows point to grossly remodeled cortical zones centered on radial artery (blue rings). At left, overall appearance of this double KO (c) is comparable to a WT; for this single megalin KO (e), fewer areas with gross remodeling are seen. All identical scale bars at 500 microm.

Supplementary figure 7



RT-PCR. Megalin ablation in Ctns KO kidneys appears to prevent loss of cubilin, NaPi-IIa and SGLT-2 mRNAs (males, blue squares; females, red disks).[1, 2]

Supplementary References

1. Gaide Chevronnay, H.P., et al., *Time course of pathogenic and adaptation mechanisms in cystinotic mouse kidneys*. J Am Soc Nephrol, 2014. **25**(6): p. 1256-69.
2. Dupasquier, S., et al., *Validation of house-keeping gene and impact on normalized gene expression in clear cell renal cell carcinoma: critical reassessment of YBX3/ZONAB/CSDA expression*. BMC Mol Biol, 2014. **15**: p. 9.